

# Damping system for torsion modes of mirror isolation filters in TAMA300

**Yuta ARASE<sup>1</sup>, Ryutaro TAKAHASHI<sup>2</sup>, Koji ARAI<sup>2</sup>, Daisuke TATSUMI<sup>2</sup>,  
Mitsuhiko FUKUSHIMA<sup>2</sup>, Toshitaka YAMAZAKI<sup>2</sup>, Masa-Katsu FUJIMOTO<sup>2</sup>,  
Kazuhiro AGATSUMA<sup>3</sup>, Noriyasu NAKAGAWA<sup>3</sup>**

<sup>1</sup> Department of Astronomy, University of Tokyo, Tokyo, 113-0033, JAPAN

<sup>2</sup> National Astronomical Observatory of Japan, Mitaka, 181-8588, JAPAN

<sup>3</sup> Institute for Cosmic Ray Research, University of Tokyo, Kashiwa, 277-8582, JAPAN

E-mail: arase.yuta@nao.ac.jp

**Abstract.** The seismic attenuation system (SAS) in TAMA300 consists of a three-legged inverted pendulum and mirror isolation filters in order to provide a high level of seismic isolation. However, the mirror isolation filters have torsion modes with long decay time which disturb the interferometer operation for about half an hour if they get excited. In order to damp the torsion modes of the filters, we constructed a digital damping system using reflective photosensors with a large linear range. This system was installed to all of four SASs. By damping of the target torsion modes, the effective quality factors of the torsion modes are reduced to less than 10 or to unmeasurable level. This system is expected to reduce the inoperative period by the torsion mode excitation, and thus will contribute to improve the duty time of the gravitational wave detector.

## 1. Introduction

Seismic attenuation systems (SASs) were installed to all test masses of the TAMA300 gravitational wave detector [1] in order to provide high level of seismic isolation [2, 3]. The SAS is a hybrid system of passive isolation and active damping. As shown in Figure 1, the passive part consists of the components as listed below:

- a three-legged inverted pendulum (IP). A function of the IP is pre-filtering of low-frequency seismic noise in the two horizontal translation degrees of freedom and a rotational degree of freedom [4].
- mirror isolation filters formed by Filter-0, Filter-1, and a mirror suspension. Filter-0 is a vertical isolation spring, called MGAS [5], that is fixed on the top of the IP. Filter-1 is also an MGAS filter suspended from Filter-0. The mirror suspension is a multiple pendulum suspended from Filter-1 by a single wire.

One of the active damping system is an inertial damping, which was employed to suppress mechanical resonances in a low frequency band. For this purpose, the motion of the top of the IP is detected by a triplet of accelerometers [6] aligned in a symmetrical arrangement and actuated by actuators [7].

However, it is difficult to use the inertial damping system alone to suppress some of the torsion modes of the mirror isolation filters. This is because the torsional motion of the filters does not appear in the top of the IP as they are decoupled. The yaw mode of the IP, which is at 550 mHz, is much stiffer than the torsion modes of the filters, which are at 40 mHz and 80 mHz. These torsion modes have long decay times due to their high quality factors ( $\sim 100$ ) and the low resonant frequencies. Once these modes are excited, the angular amplitude of the mirror grows to almost ten mrad. This large mirror motion utterly exceeds the range of mirror actuators and thus disturbs interferometer operation for about half an hour.

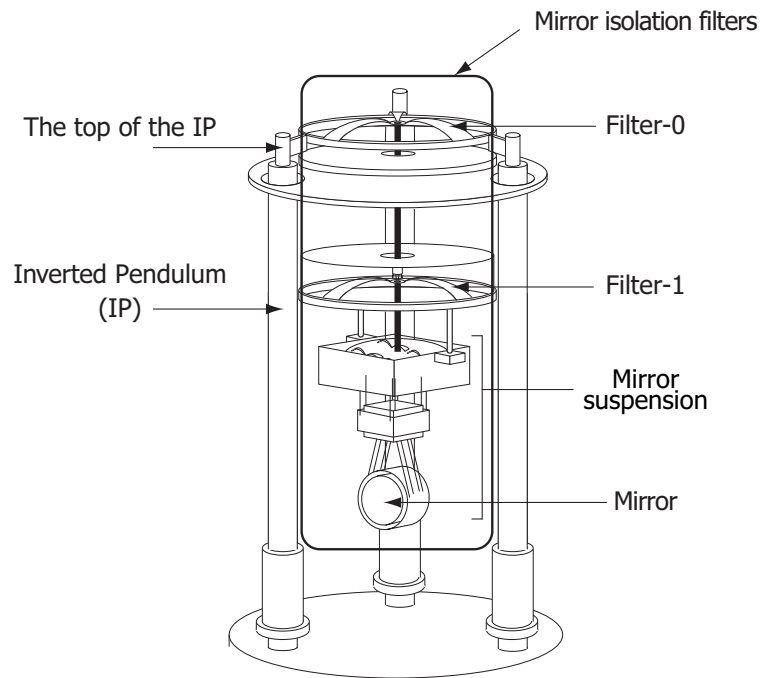


**Figure 1.** Passive springs of the TAMA SAS. Mirror isolation filters are suspended from the top of an inverted pendulum(IP) by a single wire.

In order to solve this problem, we constructed an active damping system for the torsion modes independently from the inertial damping system. Our aim is to reduce the decay times of the torsion modes to less than a few minutes. This corresponds to the effective quality factors of these modes being less than 10. We developed such a system using differential reflective photosensors and digital control filters. From the next section, we describe details of this control system and results of the performance evaluations.

## 2. Torsion mode control system

### 2.1. Control topology

The concept of our control system is shown in Figure 2. The angular motion of Filter-1 is sensed by differential detection of two photosensor outputs. Sensing at Filter-1 enables us to damp both of the torsion modes, i.e. the primary mode at about 40 mHz and the secondary mode at about 80 mHz. This is because Filter-1 and the mirror suspension, which are suspended by a single wire, are considered as a coupled oscillator. The three coil-magnet-pair actuators for the inertial damping developed for the SAS [7] are also used for the torsion mode damping. Digital filters are employed in order to realize this low-frequency control system.

In the following sections, we describe details of the angular sensor and the digital servo.

### 2.2. Angular sensor

The head of the angular sensor has been attached on a frame of the SAS against Filter-1, as shown in Figure 3. Since the frame of the SAS stands on the ground, the output signal corresponds to angular motion of Filter-1 relative to the ground. The sensor head is formed by two reflective photosensors which are placed with a separation of 24 cm. In order to minimize contamination of the translational motion of Filter-1, the two photosensor outputs are differentially amplified, and their gains are also balanced. As a result, contribution of the translational motion is reduced by a factor of about 100 in comparison to the raw output of each photosensor.

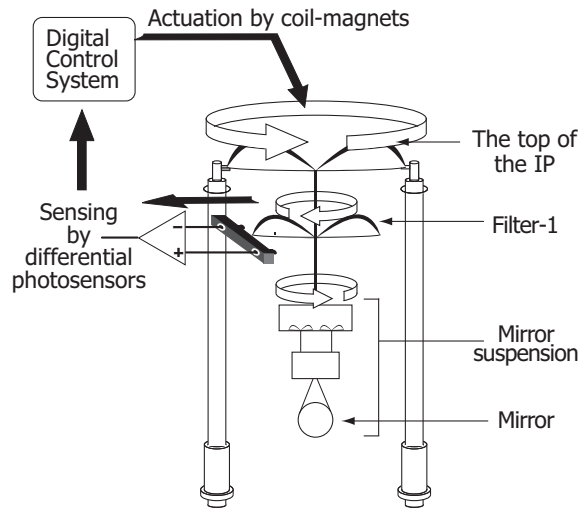


**Figure 2.** Conceptual diagram of the torsion mode control system.

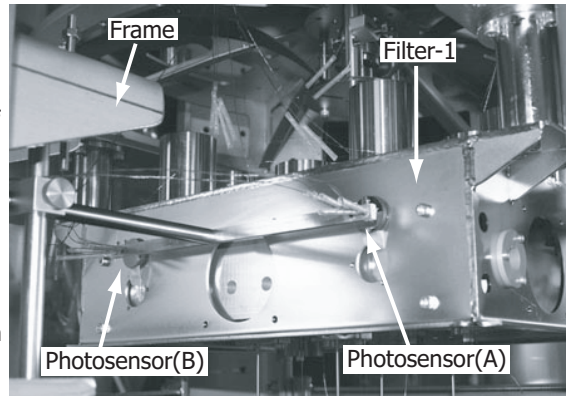


**Figure 3.** Setup of the differential reflective photosensors. Two photosensors are fixed on a bar, which in turn is fixed on the frame of the SAS standing on the ground.

Each reflective photosensor, which is a set of a LED (Honeywell SE3470) and a photodiode (HAMAMATSU S5821) separated 10 mm, has a large linear range of 5 mm corresponding to an angular range of 20 mrad. The sensor noise level of about  $10^{-6} \text{ rad}/\sqrt{\text{Hz}}$  at the target frequency band was measured (Fig. 4), by placing the photosensor and a fixed mirror on an optical table. The result of this table-top measurement suggests that these photosensors have enough sensitivity to sense the target torsion modes.

### 2.3. Servo design of the digital control filters

In order to achieve the desired damping, an open loop gain of more than 10 is required for each torsion mode. In addition, it is necessary to make the control gain above 100 mHz as low as possible, in order to avoid undesirable noise injection to the system.

With the digital control filters using LabVIEW, such a low frequency control system has been realized with high precision pole/zero placements as shown in Table 1.

The open loop transfer function of the servo was measured and compared with the one which was calculated from the filter shape and the measured actuator-sensor response (Fig. 5). This indicates that a stable servo, as being designed, is realized. The phase margins are more than 30 degree at all unity gain frequencies. There is a 180-degree phase advance at 70mHz owing to the resonance of the lower stage. This is one of the advantages of sensing at Filter-1 to ensure the stability of the servo loop. In addition, the control gain above 100 mHz decreases to less than 0.3. Note that the gains at the torsion mode resonances could not be measured due to poor resolution of the measurements. Therefore the performance of the damping servo should have been confirmed by ring-down measurements, as described in the next section.

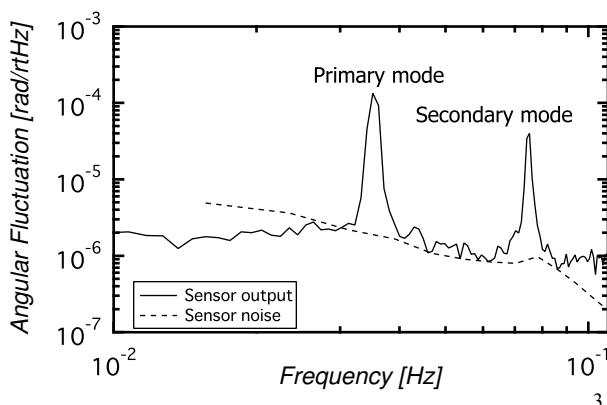


**Figure 4.** Noise level of the angular sensor. The dotted line is the sensor noise and the solid line is the power spectrum density of the measured angular fluctuation of Filter-1 without the control. The two peaks are the torsion modes to be damped.

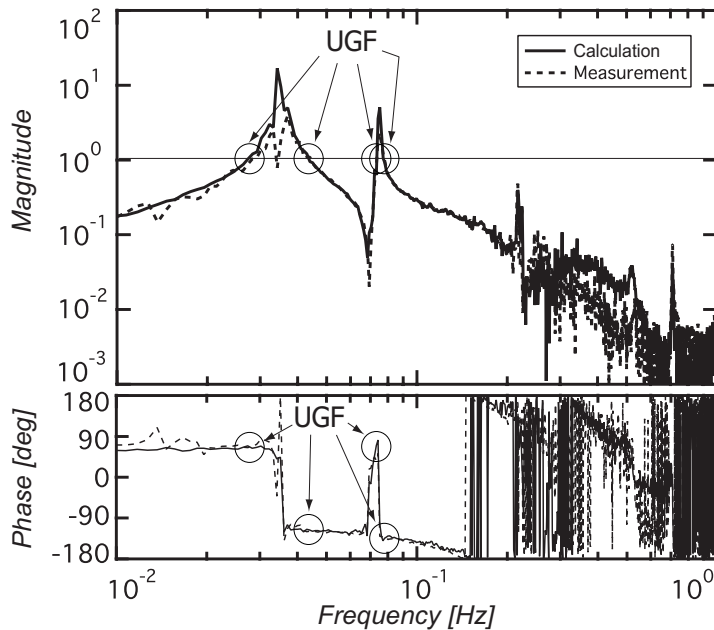


**Table 1.** Position of the pole/zero at the digital filters.

	Frequency	Quality factor
zero	0.004	
zero pair	0.2168	5.
pole pair	0.2168	2.
pole pair	0.3	0.7
zero pair	0.5178	10.
pole pair	0.5178	1.
pole	10.	

**Figure 5.** Measured (dotted) and calculated (solid) open loop transfer functions of the servo. The calculated gain is obtained from the filter shape and the measured actuator-sensor response.

### 3. Experimental results

The torsion mode control systems were installed to all of four SASs of TAMA300. In order to confirm the effect of the damping system, ring-down measurements were performed. In this experiment, the time series data of the sensor output are recorded, while the torsion modes are excited by adding an impulse to the top of the IP. The recorded data is segmented into chunks of 27 second length. An amplitude of the target mode is obtained from the Fourier component of each chunk.

The obtained time series of the mode amplitude is fitted with an exponential decay and a stationary component by sensing noise, assuming non-correlation between them. The period in which the mode amplitude becomes  $1/e$ , was defined as the decay time  $\tau$ . From the decay time, the quality factor of the mode is calculated from the following formula:

$$Q = \pi f_0 \tau, \tag{3.1}$$

where  $Q$  and  $f_0$  are the quality factor and the mode frequency, respectively.

Figure 6 shows the results of the ring-down experiments for the SAS for the perpendicular input test mass, with and without the active damping. The effect of the damping was apparently observed. In this experiment, the excitation of 3 mrad was applied, while the amplitude was settled to the sensor noise level after 400 seconds. The effective quality factor of 8.8 was achieved when the active damping was used.

Then, the ring-down measurements were performed for all of SASs. Table 2 shows the mode frequency, the original quality factor, and the effective quality factor for each mode of each SAS. We have confirmed that the quality factors of the primary modes were suppressed below 10. For some of the secondary modes, quality factors could not be measured. Also, most of the effective quality factors could not be measured. We believe that this is because the inherent or effective quality factors were too low to be measured by the ring-down experiment. Therefore we conclude that the desired low quality factors are realized.

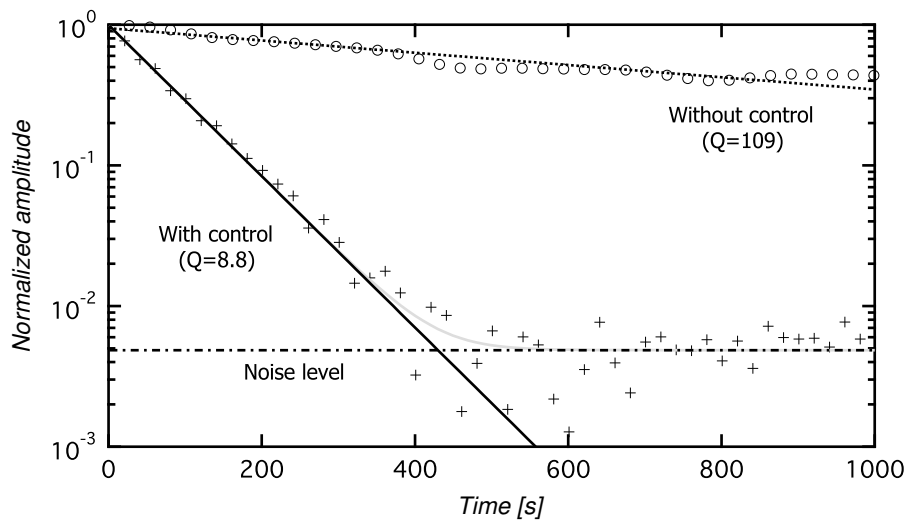


**Figure 6.** Measurement of ring-down decays for the primary torsion mode of an SAS with and without the active damping (cross and circle, respectively). The solid and dotted lines show the results of an exponential fit of each decay.

**Table 2.** Measured values of the mode frequency, the original quality factor, and the effective quality factor for each mode of each SAS. The original and effective quality factors mean the quality factors without and with the active damping, respectively. Dashes indicate that the corresponding value could not be measured. The names of the chambers, *NM* and *EM*, denote the chambers for the input and end mirrors, respectively, and the numbers '1' and '2' mean the inline and the perpendicular arm, respectively.

Primary mode			
Vacuum chamber	Frequency	original Q factor	effective Q factor
NM1	41.2 mHz	91	5.2
EM1	46.3 mHz	22	5.3
NM2	35.5 mHz	109	8.8
EM2	48.9 mHz	28	1.5
Secondary mode			
Vacuum chamber	Frequency	original Q factor	effective Q factor
NM1	86.1 mHz	313	11.6
EM1	93.1 mHz	—	—
NM2	74.9 mHz	378	—
EM2	89.7 mHz	—	—

#### 4. Summary

We have constructed an active control system for the torsion modes, which have long decay times and disturb the interferometer operation. Differential sensing with two photosensors and a digital control system were used to realize this control at low frequency. The quality factors of the torsion modes were measured by ring-down experiments. The result indicates that the effective quality factors are reduced to 10, or so low, that some of them could not be measured by the ring-down experiment. The resultant decay time is shorter than 2 minutes. Consequently, we expect that this system reduces the inoperative period of the interferometer, and thus will contribute to improving the duty time of the detector.

**References**

- [1] Ando M and TAMA collaboration 2005 *Class. Quantum Grav.* **22** S881–89
- [2] Márka S *et al* 2002 *Class. Quantum Grav.* **19** 1605–14
- [3] Takamori A *et al* 2002 *Class. Quantum Grav.* **19** 1615–21
- [4] Takamori A *et al* 2007 *Nucl. Instr. and Meth. A* **582** 683–92
- [5] Cella G, Sannibale V, DeSalvo R, Márka S and Takamori A 2005 *Nucl. Instr. and Meth. A* **540** 502–19
- [6] Bertolini A *et al* 2006 *Nucl. Instr. and Meth. A* **556** 616–23
- [7] Wang C, Tariq H, DeSalvo R, Iida Y, Márka S, Nishi Y, Sanibale V and Takamori A 2002 *Nucl. Instr. and Meth. A* **489** 563–69